

The statistical distribution of nearbed wave orbital velocity in intermediate coastal water depth

Zai-Jin You *

Coastal Unit, Department of Environment and Climate Change, Locked Bag 1002, Dangar, NSW 2309, Australia

ARTICLE INFO

Article history:

Received 12 December 2008
Received in revised form 25 February 2009
Accepted 6 April 2009
Available online 8 May 2009

Keywords:

Irregular wave
Wave orbital velocity
Velocity distribution
Gaussian
Rayleigh
Weibull

ABSTRACT

The statistical distribution of wave orbital velocity in intermediate coastal water depth has been quantitatively determined from the comprehensive field velocity data collected near the seabed in this study. Two ocean ADV current meters, which were mounted at 0.5 m above the seabed on two separate stainless steel tripods sitting on the seabed, were used to measure instantaneous water particle velocities at a 2 Hz sampling rate for 17.07 min every hour in two coastal water depths of 11 m and 23 m in nine field deployments over a period of 2 years. The zero-crossing method is applied to analyse the field velocity data collected in each field deployment to obtain a large sample of wave orbital velocity amplitudes of individual waves. Based on the collected field velocity data, it is found that the histogram of instantaneous wave orbital velocities perfectly follows the Gaussian distribution as commonly assumed, while the histogram of wave orbital velocity amplitudes is less accurately described by the Rayleigh distribution than the modified Rayleigh and the Weibull distribution. It is also found that large orbital velocity amplitudes are generally overestimated by the Rayleigh distribution, but well predicted by the modified Rayleigh and the Weibull distribution. The expected value of maximum orbital velocity in a velocity record of finite size is also derived from the three distributions and found to agree well with the present field data.

© 2009 Elsevier B.V. All rights reserved.

1. Introduction

Irregular wave orbital velocities are induced near the seabed as ocean surface waves propagate from deep water to intermediate and shallow waters. The deep water is explicitly defined as $k_0 h \geq \pi$, the shallow water as $k_0 h \leq 0.1$ and the intermediate water as $0.1 < k_0 h < \pi$ (You, 2008), where k_0 is the deepwater wave number. The nearbed orbital velocity interacts with the seabed resulting in frictional dissipation of wave energy, mobilization of bed sediment, formation of different bed forms, and modification of wave bottom shear stress (You, 2005). Thus, the study of the nearbed orbital velocity distribution is of practical importance in modelling of coastal wave hydrodynamics, scour around coastal structures, and coastal sediment transports.

However, only a few studies have been undertaken to study the wave orbital velocity distribution. Sultan (1992) measured wave orbital velocities near the bottom in a laboratory wave flume with a laser Doppler velocity meter. It was found that the distribution of instantaneous orbital velocities obeys the Gaussian distribution, and the distribution of wave orbital velocity amplitudes approximately follows the Rayleigh distribution. It was also found that the Gram–Charlier distribution is less effective than the Gaussian distribution in fitting to the measured instantaneous orbital velocities, while a modified form of the

Rayleigh distribution, the Beta–Rayleigh distribution, agrees better with the measured orbital velocity amplitudes than the Rayleigh distribution. Sultan (1992) and Sultan and Hughes (1993) all recommended to undertake further field studies to broaden the data range from which the statistical distributions were derived. Song and Wu (2000) studied the statistical distributions of horizontal and vertical instantaneous orbital velocities based on a second-order random wave theory. The wave spectrum of Donelan and Pierson (1987) was used to estimate the parameters of the distributions. It was found that the distribution of vertical orbital velocities obeys the Gaussian distribution under the second-order random wave approximation, while the distribution of horizontal orbital velocities deviates from the Gaussian distribution when water depth becomes less than 10 m. Unfortunately, no field data were applied to confirm their findings. Wiberg and Sherwood (2008) studied the distribution of wave orbital velocity amplitude based on their 2-month field data collected in a 40 m water depth in Hudson Shelf Valley, and found that the histogram of wave orbital velocity amplitudes well obeys the Rayleigh distribution. It was then concluded that the distribution of the amplitude of a narrow-banded and Gaussian random process, such as surface waves and orbital velocities, follows a Rayleigh distribution. However, none of all the studies has directly compared the measured orbital velocities U_Q with those calculated from the proposed distributions, where U_Q is averaged from the n largest orbital velocities out of m wave orbital velocity amplitudes and $Q = n/m$. The estimation of U_Q is one of the main purposes for the study of wave orbital velocity distribution.

* Tel.: +612 4904 2592; fax: +612 4904 2598.
E-mail address: bob.you@environment.nsw.gov.au.

As a result, it is often assumed that the distribution of wave orbital velocity amplitude is the same as that of wave height. Longuet-Higgins (1952) first applied the Rayleigh distribution to study the distribution of deepwater wave height in a narrow-banded sea. The Rayleigh distribution was then modified by Cartwright and Longuet-Higgins (1956) and Longuet-Higgins (1980) by introducing a scale parameter to account for finite wave spectral bandwidth. A more general distribution, the Weibull distribution, was also proposed by Forristall (1978) to study the distribution of ocean wave heights in the Gulf of Mexico. The distributions of the Rayleigh, the modified Rayleigh and the Weibull are three commonly-used probability distribution functions for the description of random ocean wave height distribution.

In this study, the statistical distribution of nearbed orbital velocity amplitude will be quantitatively determined from the comprehensive field velocity data collected in two coastal water depths of 11 m and 23 m in nine separate field developments over a period of 2 years, and then compared with three commonly-used distributions of the Rayleigh, the modified Rayleigh and the Weibull. Several useful formulas are also derived from the three distributions to calculate the characteristic orbital velocities U_Q and U_p , the expected value of maximum orbital velocity $E(U_{max})$, and finally compared with the field data collected in this study.

2. Data collection

2.1. Study sites

The field data were collected simultaneously at two sites off MacMasters Beach on the NSW Central coast (see Fig. 1). The beach is 1.5 km long and located between two high sandstone headlands. The orientation of the beach is south easterly, the dominant wave direction of the NSW coast. The offshore morphology of the beach is relatively simple and there is no offshore reef (Evans et al., 2000). The inner site was located in a water depth of 11 m and the outer site in 23 m. The bed sediment at the two sites was fine, with median grain size of $d_{50} \approx 0.2$ mm. The echo sounder and side scan sonar with DGPS were used to map the offshore bathymetry and the spatial distribution of sediment types. The deepwater waves were recorded by a directional wave rider buoy deployed permanently in water depth of 85 m off Sydney, about 120 km south of this study site. The yearly mean significant wave period $T_{1/3}$ measured by the wave-rider buoy is about 8 s. The relative water depth k_0h , which varies from 0.66 in the

inner site to 1.38 in the outer site and $0.1 < k_0h < \pi$, is intermediate (You, 2008).

2.2. Instrumentation

Two ocean Acoustic Doppler Velocimeters (ADV) were mounted on two separate stainless steel tripods to directly measure instantaneous water particle velocities and wave hydrodynamic pressures at 0.5 m above the seabed. One instrumented tripod was deployed at the inner site and the other at the outer site. The horizontal velocity components (u, v), which are measured in the compass (east–north) coordinates, were recorded at a sampling rate of 2 Hz for 17.07 min every hour at the inner site of 11 m and the outer site of 23 m, simultaneously. Nine field deployments were undertaken at the two sites over a period of 2 years, and the duration of each deployment ranges from 31 to 66 days. The sampling length of 17.07 min was designed to give 2048 or 2^{11} data points in each velocity burst in order to apply the Fast Fourier Transform to compute wave spectrum. The 2 Hz sampling rate was used to record about 10–20 velocity data points within one wave period of $T = 5$ –10 s.

3. Statistical distributions

3.1. Instantaneous orbital velocity

The instantaneous horizontal velocity components, $u(t)$ and $v(t)$, were directly measured at a 2 Hz sampling rate for 17.07 min every hour at the inner and outer sites, simultaneously. The instantaneous wave orbital velocity components, $\tilde{u}(t)$ and $\tilde{v}(t)$, can be then determined from $u(t)$ and $v(t)$ as

$$(\tilde{u}, \tilde{v}) = (u, v) - (\bar{u}, \bar{v}) \quad (1)$$

where (\bar{u}, \bar{v}) are the mean horizontal velocity components and are averaged over one sampling length of 17.04 min. Note that the wave orbital velocities (\tilde{u}, \tilde{v}) calculated from Eq. (1) also contain the turbulent velocity component. The root-mean-square velocities $(\tilde{u}_{rms}, \tilde{v}_{rms})$ computed from the instantaneous orbital velocities (\tilde{u}, \tilde{v}) are expected to slowly vary from one burst to another one. The velocity bursts, which have extremely large or small values of \tilde{u}_{rms} or \tilde{v}_{rms} , will be excluded for the computation of the orbital velocity distribution. The measured abnormal velocities were found during the coastal

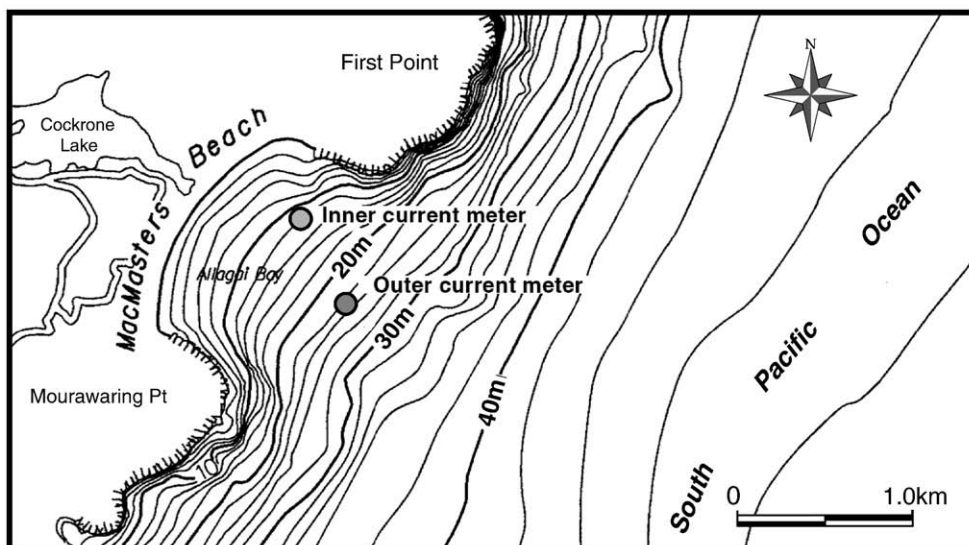


Fig. 1. Locations of the inner and outer study sites at MacMasters Beach.

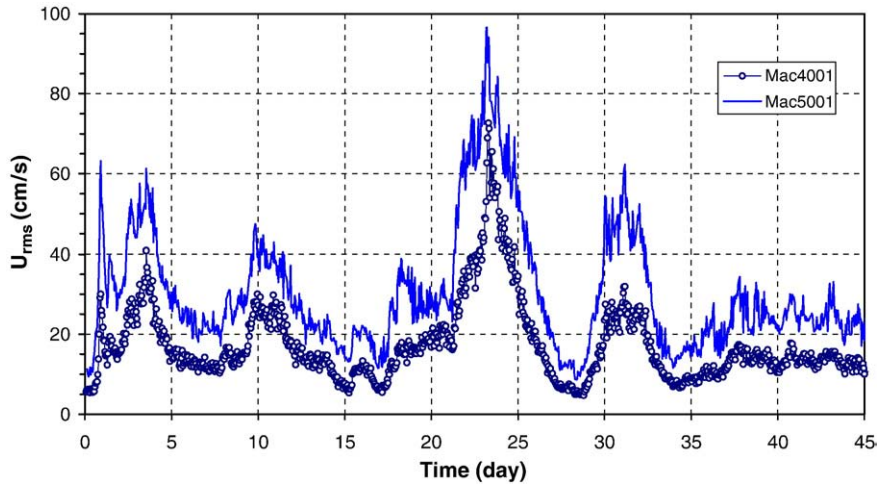


Fig. 2. The rms wave orbital velocities U_{rms} , measured in the inner and outer sites.

storms that may generate high suspended sediment concentrations and possibly entrained air bubbles near the seabed to affect the ADV velocity readings.

Fig. 2 shows an example of the rms wave orbital velocities measured in the inner and outer sites of Mac4001 and Mac5001, where $U_{rms} = \sqrt{\tilde{u}_{rms}^2 + \tilde{v}_{rms}^2}$. The rms orbital velocities measured at the inner site are shown to be generally larger (about 1.3 times) than those at the outer site. Several coastal storm events were recorded during the deployment period of 45 days, and the largest value of U_{rms} is about 97 cm/s at the inner site, and 72 cm/s at the outer site.

The histogram of $\tilde{u}(t)$, for example, is then computed as follows: (1) computing instantaneous orbital velocities (\tilde{u}, \tilde{v}) via Eq.(1) and then the rms velocity \tilde{u}_{rms} in each velocity burst, and normalising individual orbital velocities $\tilde{u}(t)$ by \tilde{u}_{rms} , (2) ordering the normalised values of $\tilde{u}/\tilde{u}_{rms}$ from all velocity bursts and grouping the ordered values of $\tilde{u}/\tilde{u}_{rms}$ into different velocity classes, and (3) computing the histogram of $\tilde{u}/\tilde{u}_{rms}$ as

$$f(x) = \frac{1}{\Delta} \left(\frac{n}{m} \right), \tag{2}$$

where $x = \tilde{u}/\tilde{u}_{rms}$, m is the total number of wave orbital velocities, n is the number of orbital velocities falling into a velocity bin or

class, and Δ is the velocity bin width. The value of $\Delta = 0.2$ is used to divide the normalised velocity range $(-3, 3)$ into 31 velocity classes. The stationarity of the process of $x = \tilde{u}/\tilde{u}_{rms}$ may be determined by the rms velocity x_{rms} computed from individual velocity burst of 17.07 min. Since the rms velocity of the normalised orbital velocity $\tilde{u}/\tilde{u}_{rms}$ calculated from each velocity burst of 17.07 min is always equal to 1, the rms velocity of $\tilde{u}/\tilde{u}_{rms}$, which is computed from all velocity bursts, is equal to 1 as well. Thus, the process of $\tilde{u}/\tilde{u}_{rms}$ is stationary over the period of the deployment provided the process of $\tilde{u}(t)$ is stationary over each sampling period of 17.07 min.

Based on the orbital velocity data (\tilde{u}, \tilde{v}) collected for 45 days at the inner site of Mac5001, the histograms of $\tilde{u}/\tilde{u}_{rms}$ and $\tilde{v}/\tilde{v}_{rms}$ are computed from Eq. (2) and shown in Fig. 3 (A). It can be seen that the histograms of $\tilde{u}/\tilde{u}_{rms}$ and $\tilde{v}/\tilde{v}_{rms}$ are almost identical and perfectly follow the Gaussian distribution as commonly assumed. The mean of x in Fig. 3 is also calculated to study the symmetry of the histograms. It is found that the mean of x is -0.03 at the inner site and -0.01 at the outer site, and thus the histogram of $\tilde{u}/\tilde{u}_{rms}$ or $\tilde{v}/\tilde{v}_{rms}$ is generally symmetric at both the sites, where $\bar{x} = \sum x f(x)$ and $f(x)$ is a discrete probability density measured at x in Fig. 3.

For engineering applications, however, the resultant orbital velocity $\tilde{U}(t)$ in the direction θ of wave propagation is often used to

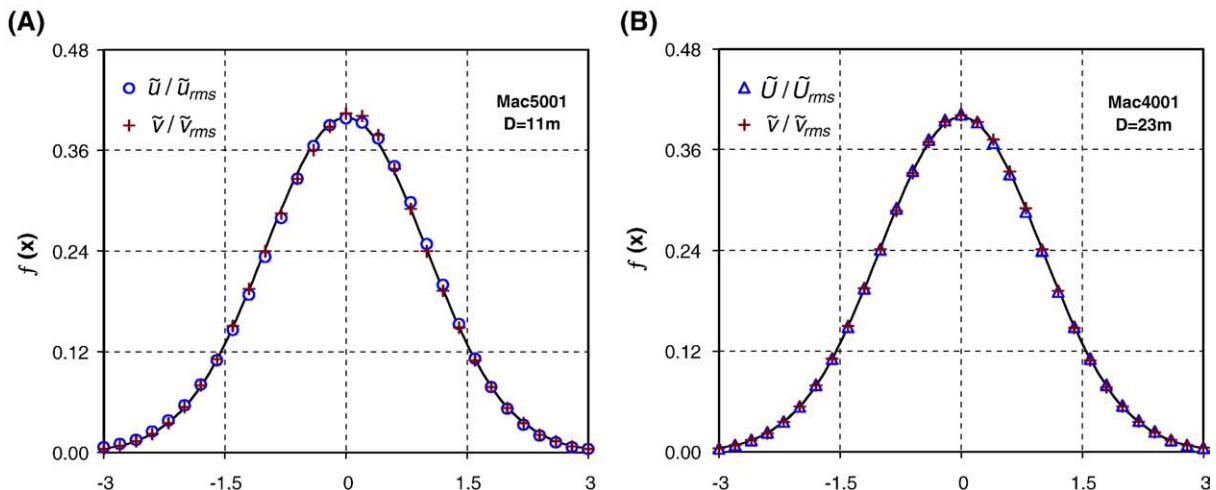


Fig. 3. The histograms of $\tilde{u}/\tilde{u}_{rms}$, $\tilde{v}/\tilde{v}_{rms}$ and $\tilde{U}/\tilde{U}_{rms}$ calculated from a large number of orbital velocity records collected at the outer site of Mac4001 and the inner site of Mac5001 are compared with the Gaussian distribution (solid line).

model wave hydrodynamics, sediment transport and scour around coastal structures. $\tilde{U}(t)$ may be expressed in terms of \tilde{u} and \tilde{v} as

$$\tilde{U}(t) = \frac{\tilde{u}}{\sin \theta} = \frac{\tilde{v}}{\cos \theta} = \tilde{u} \sin \theta + \tilde{v} \cos \theta, \quad (3)$$

where θ is measured in the compass coordinates. The wave direction θ in Eq. (3) is the mean wave direction over a sampling length of 17.07 min, during which the sea state is often assumed stationary. Based on Eq. (3), θ may be estimated from a simple formula of You and Yin (2001) as

$$\tan \theta = \pm \left(\frac{\tilde{u}_{rms}}{\tilde{v}_{rms}} \right), \quad (4)$$

where θ can be uniquely determined together with the orientation of the shoreline. It was shown in Fig. 3 of You and Yin (2001) that Eq. (4) agrees well with the field wave direction data. Since \tilde{U} in each burst is linearly proportional to \tilde{u} or \tilde{v} in Eq. (3), the value of $\tilde{U}/\tilde{U}_{rms}$ will be independent of θ in each velocity burst and consequently the histogram of $\tilde{U}/\tilde{U}_{rms}$ should be identical to that of $\tilde{u}/\tilde{u}_{rms}$ or $\tilde{v}/\tilde{v}_{rms}$. The accuracy of the calculated θ from Eq. (4) will not affect the computed pdf of $\tilde{U}/\tilde{U}_{rms}$. It is shown quantitatively in Fig. 3(B) that the pdf of $\tilde{U}/\tilde{U}_{rms}$ is indeed identical to that of $\tilde{v}/\tilde{v}_{rms}$ based on the field data collected at the outer site of Mac4001. The pdfs of $\tilde{U}/\tilde{U}_{rms}$ calculated from the other field deployments are also found to follow the Gaussian distribution as well.

3.2. Orbital velocity amplitude

In engineering practice, coastal engineers are normally concerned with orbital velocity amplitude U rather than instantaneous orbital velocity $\tilde{U}(t)$. The velocity amplitudes U of individual waves are analysed from the time-series orbital velocity $\tilde{U}(t)$ with the zero-up crossing method. The velocity amplitude U is defined here as $U = 0.5 \times (u_{max} - u_{min})$, where u_{max} and u_{min} are the maximum and minimum orbital velocities of a wave. The waves at the study sites were found generally symmetric based on the wave pressure data collected at the inner site of 11 m and the outer site of 23 m in different field deployments.

The distribution of U/U_{rms} is computed with the same method that is used to calculate the histogram of $\tilde{u}/\tilde{u}_{rms}$ in Fig. 3. The histograms and the probability distributions of U/U_{rms} are computed from a large number of velocity records collected for 45 days at the inner site of Mac5001 and the outer site of Mac4001 and shown in Fig. 4. It can be seen that the probability distributions of U/U_{rms} approximately follow the Rayleigh distribution

$$Q = \exp \left[- \left(\frac{U}{U_{rms}} \right)^2 \right], \quad (5)$$

where Q is the probability of exceeding. Eq. (5) is shown to overestimate the probability of large velocity amplitudes, eg $U > 1.5U_{rms}$. Eq. (5) can be derived from the Gaussian distribution of

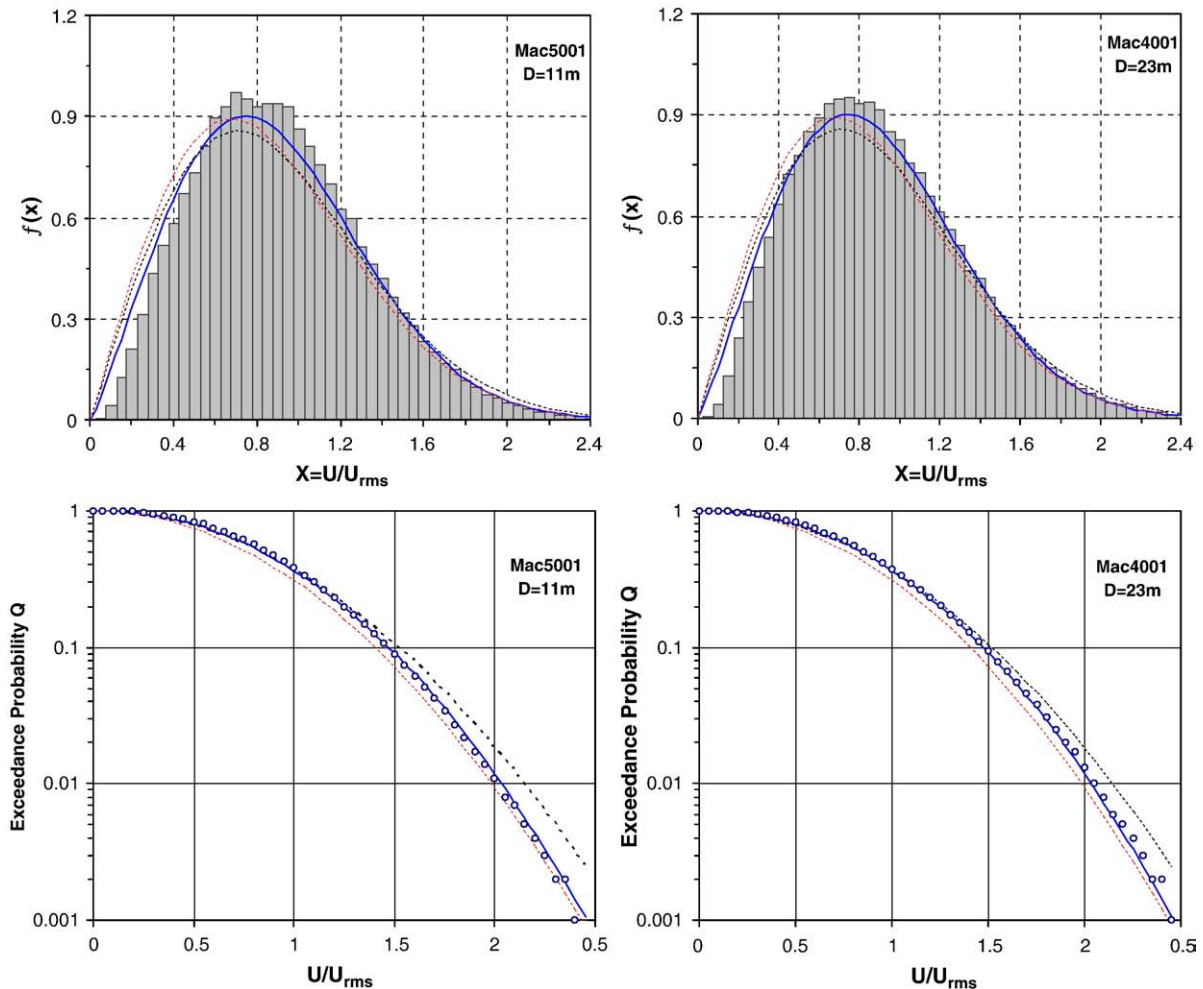


Fig. 4. The histograms and the probability distributions of U computed from the field data are compared with the Rayleigh (dotted line), the modified Rayleigh (long dashed line) and the Weibull distribution (solid line).

instantaneous orbital velocity \tilde{U} with the same method that was used by Longuet-Higgins (1952) to derive the Rayleigh distribution of wave height in a narrow-banded sea.

With introducing a scale parameter in Eq. (5), the Rayleigh distribution may be modified as

$$Q = \exp\left[-\left(\frac{U}{CU_{rms}}\right)^2\right] = \exp\left[-\left(\frac{U}{U_r}\right)^2\right], \quad (6)$$

where $C=0.925$ was determined by Longuet-Higgins (1980). The scale parameter C was initially introduced to account for finite wave spectral bandwidth (Massel and Sobey, 2000). Mathematically, the term $C \times U_{rms}$ in Eq. (6) may be considered as a reference velocity U_r that is smaller than the rms velocity U_{rms} , but larger than the mean velocity U_1 . The modified Rayleigh distribution Eq. (6) with one degree of freedom could give a better fitting to the field data than the Rayleigh distribution Eq. (5) with no degree of freedom. Eq. (6) with a newly proposed value of $C=0.96$ from this study is compared with the field data in Fig. 4. It can be seen that the modified Rayleigh distribution Eq. (6) agrees better with the field data than the Rayleigh distribution Eq. (5).

Alternatively, with introducing a shape parameter α rather than the scale parameter C in Eq. (5), the Rayleigh distribution may be also modified as

$$Q = \exp\left[-\left(\frac{U}{U_{rms}}\right)^\alpha\right], \quad (7)$$

which is also called the one-parameter Weibull distribution with one degree of freedom. The value of $\alpha=2.15$ is determined with a linear fitting method, i.e. transforming Eq. (7) into a linear equation $Y=\alpha X$ and then fitting a linear regression line through the field data points (X, Y) of Mac4001 to obtain the value of α , where $X=\ln(U/U_{rms})$ and $Y=\ln[-\ln(Q)]$. It is shown in Fig. 4 that the Weibull distribution agrees better with the field data than Eqs. (5) and (6). Forristall (1978) also proposed a two-parameter Weibull distribution to study the distribution of wave heights in the Gulf of Mexico and obtained $\alpha=2.13$. A more general two-parameter Weibull distribution with the scale and shape parameters is also fitted to the field data in Fig. 4, but found no better than the one-parameter Weibull distribution of Eq. (7).

It should be mentioned here that the field data presented in Fig. 4 include both non-storm and storm wave data. Fig. 5 shows the histogram of large velocity amplitudes ($U_{rms}>20$ cm/s) measured at the outer site of Mac4001. Only the orbital velocity records with $U_{rms}>20$ cm/s are used to calculate the histogram in Fig. 5. The rms velocities calculated from individual velocity bursts of Mac4001 are already shown in Fig. 2. The measured probability distribution of U is linearly transformed and

plotted in Fig. 5 based on the distributions of the Rayleigh, the modified Rayleigh and the Weibull, respectively. It can be seen that the distribution of storm wave orbital velocity amplitudes is almost identical to that under all wave conditions in Fig. 4, and is equally well described by the Weibull distribution. This may also confirm quantitatively that the process of $x=U/U_{rms}$ is stationary under all the coastal conditions.

4. Statistical relationships

4.1. Mean of largest velocity amplitudes

One of important engineering applications for this study is to estimate the characteristic orbital velocity U_Q , e.g. significant orbital velocity $U_{1/3}$, from a sample of wave orbital velocity amplitudes. The orbital velocity U_Q is defined as the average velocity of the n largest orbital velocities from the total number of m orbital velocity amplitudes and $Q=n/m$ is the probability of exceeding. When the probability distribution of U follows the Rayleigh distribution, U_Q can be then estimated as

$$\frac{U_Q}{U_{rms}} = \frac{\int_0^\infty U f(U) dU}{U_{rms} Q} = \sqrt{-\ln Q} + \frac{\sqrt{\pi}}{2Q} \operatorname{erfc}\left(\sqrt{-\ln Q}\right), \quad (8)$$

where $f(U)$ is the probability density function, Q is the probability of exceeding, and $\operatorname{erfc}(x)$ is the complementary error function. The relationship, $\hat{U}/U_{rms} = \sqrt{-\ln Q}$, from the Rayleigh distribution of Eq. (5) is also applied in the deviation of Eq. (8).

When $Q \rightarrow 0$, $\operatorname{erfc}(x)$ has an asymptotic solution and thus Eq. (8) may be simplified as

$$\frac{U_Q}{U_{rms}} = \sqrt{-\ln Q} + \frac{1}{2\sqrt{-\ln Q}} - \frac{(-\ln Q)^{-3/2}}{4} + \frac{3(-\ln Q)^{-5/2}}{8} \text{ for } Q \ll 1, \quad (9)$$

which is approximated up to second order. The last two terms in Eq. (9) are quite small and about 1% of the first two terms.

When $0 < Q \leq 1$, Eq. (8) may be well approximated in this study as

$$\frac{U_Q}{U_{rms}} \approx \sqrt{-\ln Q} + \frac{1}{\sqrt{-\ln Q} + \sqrt{-\ln Q} + \pi/4}, \quad (10)$$

by applying for the inequality of $\operatorname{erfc}(x)$, see Eq. (7.1.13) of Abramowitz and Stegun (1970, pp. 298). Eq. (10) has the maximum error of about 3% at $Q=0.9$ and nil error at $Q=1$ as shown in Fig. 6. Eq. (10) may be preferred over Eq. (8) for the calculation of U_Q in engineering applications because Eq. (10) is much more easily calculated with a hand

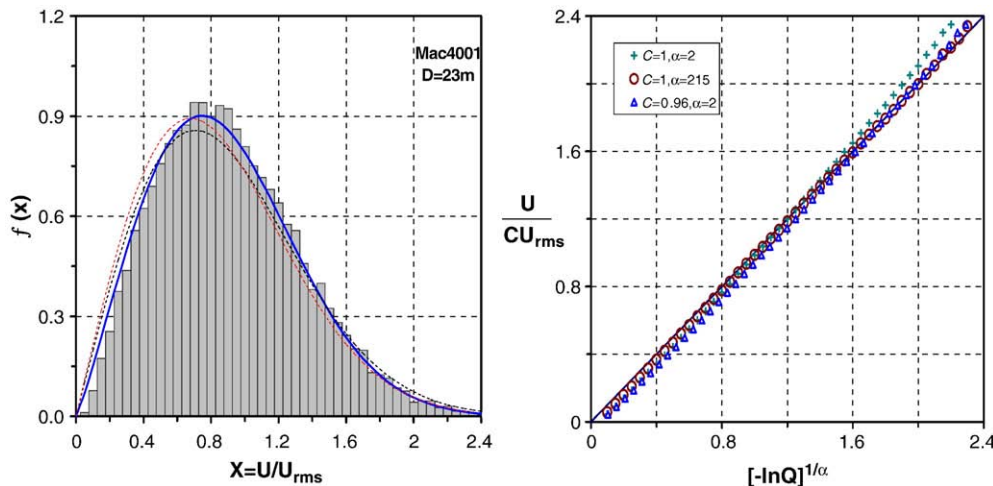


Fig. 5. The histogram of storm wave orbital velocity amplitudes is compared with the pdfs of the Rayleigh (dotted line), the modified Rayleigh (long dashed) and the Weibull distribution (thick line), and the measured probability distribution is linearly transformed and compared with Eq. (5) (+), Eq. (6) (Δ) and Eq. (7) (\circ).

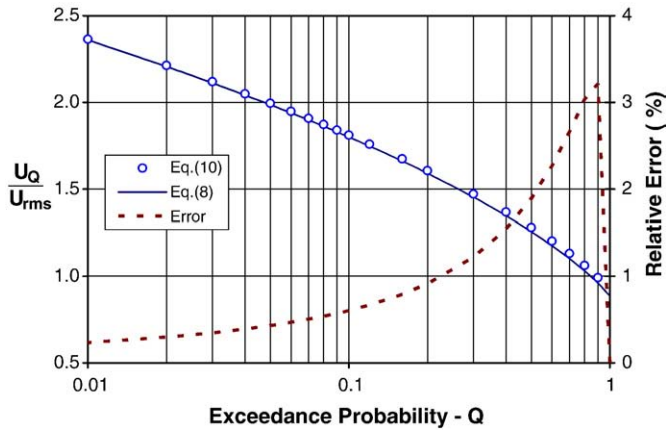


Fig. 6. The relative errors introduced when Eq. (8) is approximated to Eq. (10).

calculator than Eq. (8). Also note that Eq. (9) is a good approximation of Eq. (8) only when Q is quite small (e.g. $Q < 0.1$), while Eq. (10) is valid for all values of Q .

Similarly, U_Q can also be derived from Eq. (6) of the modified Rayleigh distribution as

$$\frac{U_Q}{U_{rms}} = C \times \left[\sqrt{-\ln Q} + \frac{\sqrt{\pi}}{2Q} \operatorname{erfc}(\sqrt{-\ln Q}) \right], \quad (11)$$

and from Eq. (7) of the Weibull distribution as

$$\frac{U_Q}{U_{rms}} = (-\ln Q)^{1/\alpha} + \frac{1}{\alpha Q} \Gamma(1/\alpha, -\ln Q), \quad (12)$$

where $\Gamma(a, x)$ is the upper incomplete gamma function and is more difficultly evaluated than $\operatorname{erfc}(x)$ of the complementary error function. Eqs. (11) and (12) all reduce to Eq. (8) when $\alpha = 2$ and $C = 1$.

When $Q \rightarrow 0$, $\Gamma(a, x)$ has an asymptotic solution and Eq. (12) may be simplified as

$$\begin{aligned} \frac{U_Q}{U_{rms}} = & (-\ln Q)^{\frac{1}{\alpha}} + \frac{(-\ln Q)^{\frac{1}{\alpha}-1}}{\alpha} + \frac{(-\ln Q)^{\frac{1}{\alpha}-2}}{\alpha} \left(\frac{1}{\alpha} - 1 \right) \\ & + \frac{(-\ln Q)^{\frac{1}{\alpha}-3}}{\alpha} \left(\frac{1}{\alpha} - 1 \right) \left(\frac{1}{\alpha} - 2 \right) \text{ for } Q \ll 1, \end{aligned} \quad (13)$$

which is also approximated up to second order. The last two terms in Eq. (13) is about 1% of the first two terms and may be neglected. Eq. (13) will reduce to Eq. (9) when $\alpha = 2$.

Fig. 7 shows the comparison of the measured values of U_Q/U_{rms} with those computed from the Rayleigh of Eq. (5), the modified Rayleigh of Eq. (6) with $C = 0.96$ and the Weibull distribution of Eq. (7). It can be seen that the Rayleigh distribution overestimates the distribution of large velocity amplitudes, while the Weibull distribution gives the best fitting to the field data. For engineering applications, however, the modified Rayleigh distribution may be preferred to the Weibull distribution for the calculation of U_Q in terms of its simplicity and accuracy.

4.2. Mean of smallest velocity amplitudes

For some engineering applications, we may be also interested in the characteristic orbital velocity U_p that is averaged from the k smallest velocity amplitudes out of the total number of m orbital velocity amplitudes and $P = k/m$ is the cumulative probability. For example, in studying the stability of an offshore spoil ground, we often want to know the percentage of time during which the spoil ground is stable or the characteristic wave nearbed orbital velocity U_p (eg $P = 1/3$) is always less than or equal to the threshold velocity of sediment motion on the spoil ground. The orbital velocity U_p can be derived from Eq. (6) of the modified Rayleigh distribution as

$$\frac{U_p}{U_{rms}} = \frac{\int_0^{\hat{U}} U f(U) dU}{U_{rms} P} = C \left[-\sqrt{-\ln Q} \left(\frac{Q}{P} \right) + \frac{\sqrt{\pi}}{2P} \left[1 - \operatorname{erfc}(\sqrt{-\ln Q}) \right] \right], \quad (14)$$

where $\hat{U}/U_{rms} = \sqrt{-\ln Q}$ is also used and $P = 1 - Q$, and from Eq. (7) of the Weibull distribution as

$$\frac{U_p}{U_{rms}} = -(-\ln Q)^{1/\alpha} \left(\frac{Q}{P} \right) + \frac{1}{\alpha P} [\Gamma(1/\alpha) - \Gamma(1/\alpha, -\ln Q)]. \quad (15)$$

Eqs. (14) and (15) reduce to one derived from the Rayleigh distribution when $C = 1$ and $\alpha = 2$.

Fig. 8 shows the comparison of the measured values of U_p/U_{rms} and U_Q/U_{rms} in Mac1001 and Mac2001 and those calculated from Eqs. (14) and (15) with the same values of $\alpha = 2.15$ and $C = 0.96$. The field data of Mac2001 and Mac1001 were collected at the inner site of 11 m and the outer site of 23 m and the length of the data is about 43 days. It can be seen that the measured values of U_p/U_{rms} are slightly underestimated by both the Weibull and modified Rayleigh distributions. This may be because the inclusion of the turbulent velocity in the value of U in Eq. (1) could significantly increase U when U is quite small (e.g. $P < 0.1$), but would become insignificant when U is quite large. This may explain why

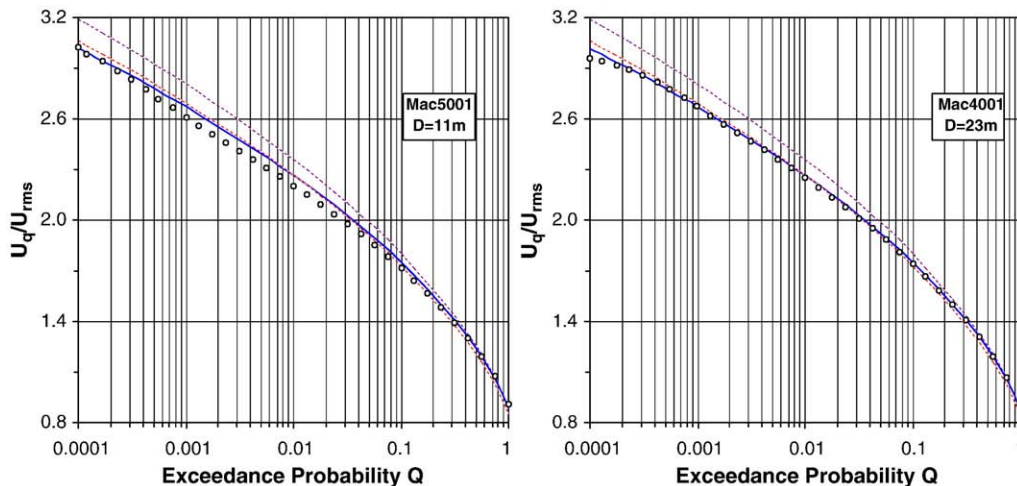


Fig. 7. The values of U_Q/U_{rms} measured in Mac4001 and Mac5001 are compared with those calculated from Eq. (8) of the Rayleigh (dotted line), Eq. (11) of the modified Rayleigh (long dashed line) and Eq. (12) of the Weibull (solid line).

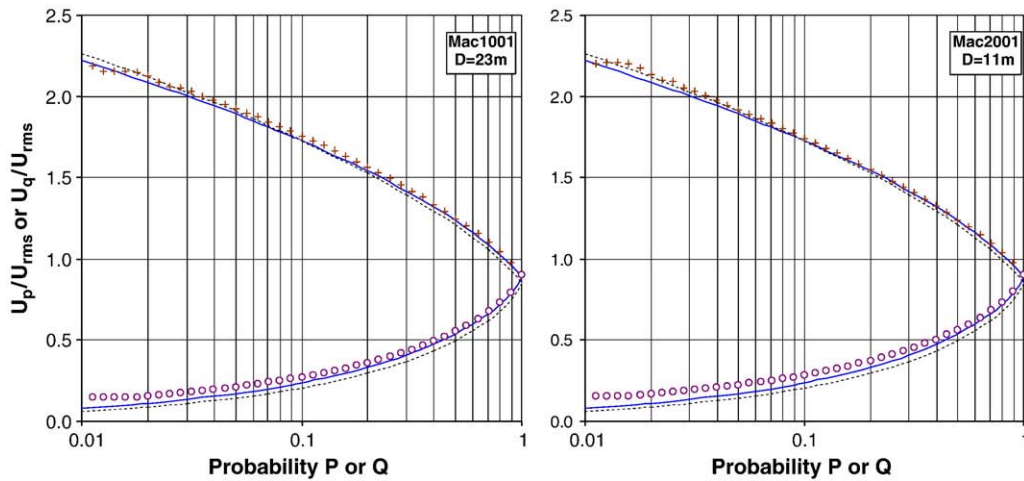


Fig. 8. The values of U_p/U_{rms} (\circ) and U_Q/U_{rms} ($+$) measured in Mac1001 and Mac2001 are compared with those calculated from the modified Rayleigh (dotted line) and from the Weibull (solid line).

the Weibull distribution slightly overestimates the small values of U_p , but gives a good prediction of the large values of U_p in Fig. 8. The Weibull distribution with $\alpha = 2.15$ give a slightly better fitting to the field data than the modified Rayleigh distribution.

4.3. Expected value of maximum velocity amplitude

Another important engineering application for this study is to estimate the expected value of maximum orbital velocity amplitude U_{max} in a velocity record of finite size N . The maximum orbital velocity amplitudes in different velocity records with the same size N are expected to be different, but may follow a certain statistical distribution. The cumulative probability that all N orbital velocity amplitudes in a velocity record of finite size N shall be less than U_{max} may be estimated from the N th order statistics as

$$P = (1 - \psi)^N = \left\{ 1 - \exp \left[- \left(\frac{U_{max}}{U_{rms}} \right)^2 \right] \right\}^N, \tag{16}$$

where ψ is the probability for any one of the N velocity amplitudes being less than U_{max} and is assumed to follow the Rayleigh

distribution and U_{rms} is the rms velocity of the N orbital velocity amplitudes. The probability ψ may be also estimated from the modified Rayleigh or the Weibull distribution. The pdfs of U_{max} with different values of N , which are derived from Eq. (16), are shown in Fig. 9(A). It can be seen that the pdf of U_{max} is asymmetric and becomes narrowly distributed with increasing N . The most probable value of U_{max} , at which the probability density function $f(x)$ is maximum, is also shown to increase with N . When N is quite large (e.g. $N > 20$), Eq. (16) may be approximated as

$$P(x) = \exp \left[- \exp(x_0^2 - x^2) \right] \text{ or } f(x) = 2x \exp \left[(x_0^2 - x^2) - \exp(x_0^2 - x^2) \right], \tag{17}$$

where $x = U_{max}/U_{rms}$ is the normalised maximum velocity amplitude and x_0 is a reference velocity and calculated as $x_0 = U_0 / U_{rms} = \sqrt{\ln N}$ via Eq. (5) of the Rayleigh distribution. The identity, $(1 + x/N)^N = \exp(x)$ for $N \rightarrow \infty$, is also used in the derivation of Eq. (17). The comparison of Eqs. (16) and (17) is shown in Fig. 9(B) with different values of N . It can be seen that Eq. (16) can be well approximated by Eq. (17) when $N \geq 20$.

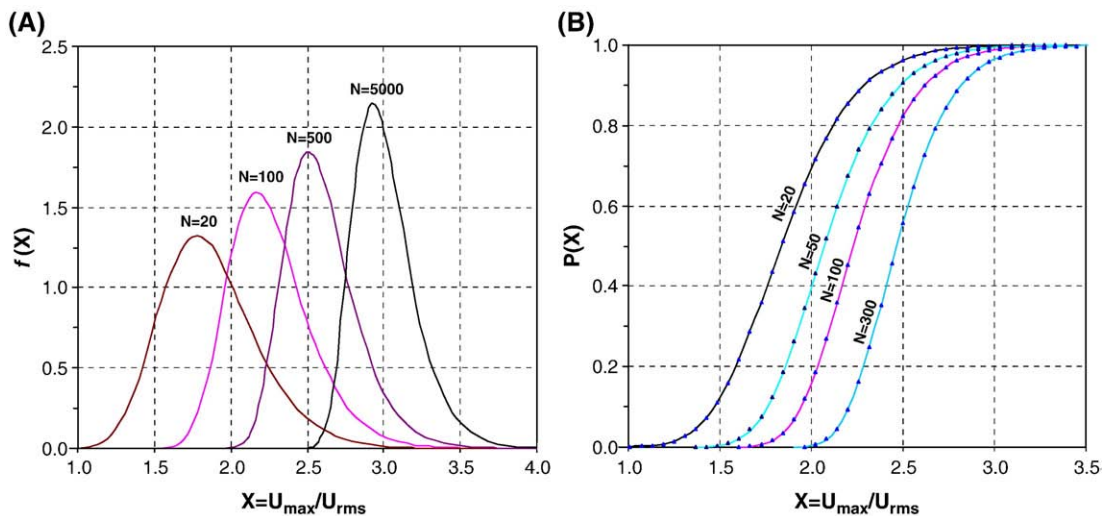


Fig. 9. [A] The pdfs of U_{max} with different values of N are calculated from Eq. (17), and [B] The probability distribution of U_{max} calculated from Eq. (16) [triangles] is compared with that from Eq. (17) [solid lines].

Now, the expected value of U_{max} , denoted by $E(U_{max})$, can be estimated from Eq. (17) as

$$\begin{aligned} \frac{E(U_{max})}{U_{rms}} &= \int_0^\infty xf(x)dx = -\int_0^\infty (x_0^2 - \ln\alpha)^{0.5} \exp(-\alpha)d\alpha \\ &\approx \int_0^\infty x_0 \left(1 - \frac{\ln\alpha}{2x_0} - \frac{(\ln\alpha)^2}{8x_0^3} \right) \exp(-\alpha)d\alpha \\ &= x_0 + \frac{\gamma}{2x_0} - \frac{(\gamma^2 + \pi^2/6)}{8x_0^3} \end{aligned} \tag{18}$$

where $x_0 = \sqrt{\ln N}$ and γ is Euler's constant ($=0.5772$). In the deviation of Eq. (18), the variable x is replaced by a new variable, $\alpha = \exp(x_0^2 - x^2)$, and the upper and lower limits ($\infty, 0$) of x are then changed to $(0, N)$ of α . Because the integrand, $x \exp(-\alpha)$, decays rapidly to zero at $\alpha > 6-10$, the lower and upper limits $(0, N)$ of α may then be written as $(0, \infty)$ in Eq. (18) provided $N \geq 20$. The term $(x_0^2 - \ln \alpha)^{0.5}$ in Eq. (18) is expanded as a binomial series of up to second order and the following identities have also been used

$$\gamma = -\int_0^\infty \ln\alpha \exp(-\alpha)d\alpha = 0.5772 \text{ and } \int_0^\infty (\ln\alpha)^2 \exp(-\alpha)d\alpha = \frac{\pi^2}{6} + \gamma^2. \tag{19}$$

It should be noted here that **Longuet-Higgins (1952)** also derived a formula similar to Eq. (18) for calculation of the expected value of maximum wave height in a sample of finite size N , but Eq. (18) has been derived differently from Eq. (59) of **Longuet-Higgins (1952)**.

When Eq. (6) of the modified Rayleigh distribution is substituted in Eq. (18), $E(U_{max})$ may be derived as

$$\frac{E(U_{max})}{U_{rms}} = C \times \left[x_0 + \frac{\gamma}{2x_0} - \frac{(\gamma^2 + \pi^2/6)}{8x_0^3} \right]. \tag{20}$$

Similarly, when Eq. (7) of the Weibull distribution is used in Eq. (18), $E(U_{max})$ may be also deduced as

$$\frac{E(U_{max})}{U_{rms}} = x_0 + \frac{\gamma}{\theta x_0^{\theta-1}} - \frac{(\gamma^2 + \pi^2/6)(\theta-1)}{2\theta^2 x_0^{2\theta-1}}, \tag{21}$$

which is identical to Eq. (18) or (20) when $C = 1$ and $\theta = 2$.

Fig. 10 shows the comparison of the measured individual values of U_{max} in the outer site of Mac7001 with those calculated from Eqs. (18), (20) and (21), respectively. There are 1392 data points (U_{max}, N) used for this comparison. Each velocity record of 17.07 min produces only one data point. It can be seen from **Fig. 10** that the expected values of U_{max} , which are calculated from Eq. (18) of the Rayleigh, Eq. (20) of the modified Rayleigh and Eq. (21) of the Weibull are very close to each other and all agree well with the measured mean value of U_{max} .

It is noted that the average velocity $E(U_{max})$ of n maximum orbital velocity amplitudes that are obtained from n individual velocity records with the same size N is expected to be slightly smaller than the average orbital velocity U_Q of the n largest orbital velocity amplitudes that are taken from a sample of the same n velocity records. This is because the n largest velocity amplitudes may not be evenly distributed in the n velocity records, i.e. each velocity record has one maximum velocity but may not have one largest velocity of the n ones and multiple largest orbital velocities of the n ones may occur in one velocity record, thus the average velocity $E(U_{max})$ of the n maximum orbital velocity amplitudes from the n velocity records should be smaller than the average orbital velocity U_Q of the n largest velocities from only some of the n velocity records. This difference between $E(U_{max})$ and U_Q is expected to be small when n and N become considerably large.

5. Conclusion

The statistical distribution of nearbed wave orbital velocity has been quantitatively determined from the comprehensive field velocity data collected in this study. The zero-crossing method is used to analyse the collected field velocity data to obtain wave orbital velocity amplitudes of individual waves. Based on the collected field data, it is found that the distribution of instantaneous wave orbital velocity well follows the Gaussian distribution as commonly assumed, and that the distribution of wave orbital velocity amplitudes is less accurately described by the Rayleigh distribution than the modified Rayleigh distribution and the one-parameter Weibull distribution. The Rayleigh distribution is also found to overestimate large orbital velocity U_q when $Q < 0.1$, but the modified Rayleigh and the Weibull distribution agree well with the collected field data. Several useful formulas are also derived to compute the orbital velocities U_Q and U_p and the expected value $E(U_{max})$ of maximum orbital velocity amplitude based on three commonly-used distributions of the Rayleigh, the modified Rayleigh and the Weibull. The modified Rayleigh distribution of Eq. (6) with $C = 0.96$ may be preferred over the distributions of the Rayleigh and the Weibull for the study of the nearbed wave orbital

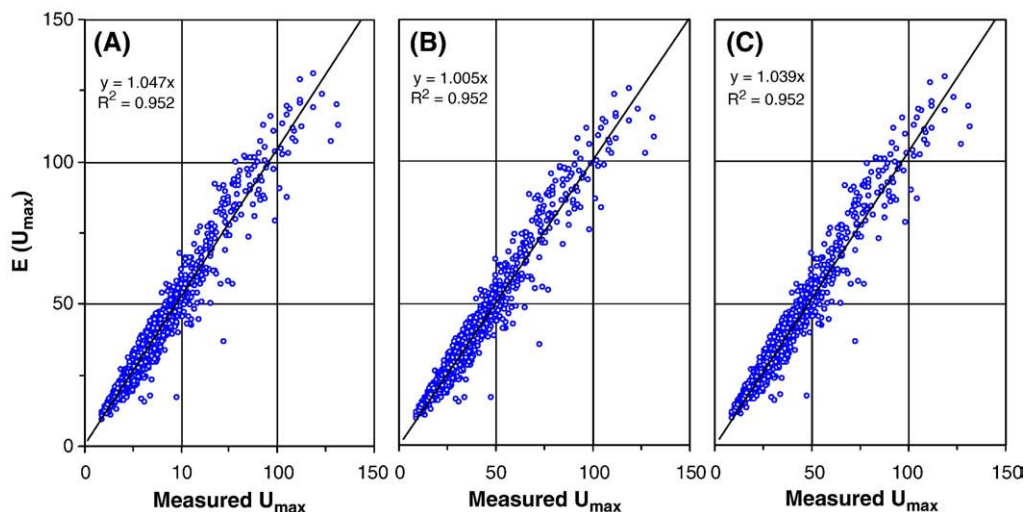


Fig. 10. The measured values of U_{max} from 1392 velocity records at the outer site of Mac7001 are compared with the expected values of U_{max} calculated from: (A) Eq. (18) of the Rayleigh, (B) Eq. (20) of the modified Rayleigh, and (C) Eq. (21) of the Weibull.

velocity distribution in intermediate coastal water in terms of its simplicity and accuracy.

References

- Abramowitz, M., Stegun, I.A., 1970. Handbook of Mathematical Functions. Dover Publications, Inc., New York.
- Cartwright, D.E., Longuet-Higgins, M.S., 1956. The statistical distribution of the maxima of a random function. Proceedings of the Royal Society of London, Series A 247, 22–48.
- Donelan, M.A., Pierson, W.J.P., 1987. Radar scattering and equilibrium granges in wind-generated waves with application of scatterometry. Journal of Geophysical Research 92, 4971–5029.
- Evans, P., Hanslow, D., Coutts-Smith, A., You, Z.J., 2000. Nearshore-inner shelf sediment exchange on the NSW central coast. Proc. 27th Int. Conf. on Coastal Eng., ASCE, pp. 3151–3164.
- Forristall, G.Z., 1978. On the statistical distribution of wave heights in a storm. Journal of Geophysical Research 83, 2353–2358.
- Longuet-Higgins, M.S., 1952. On the statistical distribution of the heights of sea waves. Journal of Marine Research 11, 245–266.
- Longuet-Higgins, M.S., 1980. On the distribution of the heights of sea waves: some effects of nonlinearity and finite band width. Journal of Geophysical Research 85, 1519–1523.
- Massel, S.R., Sobey, R.J., 2000. Distribution of the highest wave in a record. Coastal Engineering Journal 42, 153–173.
- Song, J.B., Wu, Y.H., 2000. Statistical distribution of water particle velocity below the surface layer for finite water depth. Coastal Engineering 40, 1–19.
- Sultan, N.J., 1992. Irregular wave-induced velocity in shallow water. US Army Corps of Engineering, Washington DC, Technical Report CERC-92-9.
- Sultan, N.J., Hughes, S.A., 1993. Irregular wave-induced velocities in shallow water. Journal Waterway, Port, Coast and Ocean Engineering, ASCE 119, 429–447.
- Wiberg, P.L., Sherwood, C.R., 2008. Calculating wave-generated bottom orbital velocities from surface-wave parameters. Computers and Geosciences 34, 1167–1416.
- You, Z.J., 2005. Estimation of bed roughness from mean velocities measured at two levels near the seabed. Continental Shelf Research 25, 1043–1051.
- You, Z.J., 2008. A close approximation of wave dispersion relation for direct calculation of wavelength in any coastal water depth. Applied Ocean Research 30, 113–119.
- You, Z.J., Yin, B.S., 2001. Determination of coastal wave direction in shallow water. 15th Australasian Coastal and Ocean Engineering Conference, Gold Coast, pp. 523–527.